Materials Research Bulletin 47 (2012) 2884–2887

Contents lists available at SciVerse ScienceDirect

Materials Research Bulletin

journal homepage: www.elsevier.com/locate/matresbu

Effect of Al-doped ZnO film thickness on periodic GaAs subwavelength grating structures for photovoltaic device applications

Jung Woo Leem [a], Young Min Song [b], Jae Su Yu [a,*]

[a] Department of Electronics and Radio Engineering, Kyung Hee University, Yongin 446-701, Republic of Korea
[b] Department of Materials Science and Engineering, University of Illinois at Urbana-Champaign, Urbana, IL 61801, USA

ARTICLE INFO

Article history:
Available online 25 April 2012

Keywords:
A. Nanostructures
B. Sputtering
D. Electrical properties
D. Optical properties
D. Surface properties

ABSTRACT

We investigated the effect of Al-doped zinc oxide (AZO) films with different thicknesses deposited onto periodic cone-shaped GaAs subwavelength grating (SWG) structures on their physical properties. As the AZO deposition time was increased, the surface morphology of AZO deposited GaAs SWGs was changed. These structures exhibited the surface reflection of $<\sim$6.8% at 300–1200 nm because of their effective graded index distribution between air and the GaAs substrate via the AZO deposited GaAs SWGs, producing a lowest average reflectance of $\sim$2.1% at 40 min of deposition time. With increasing the deposition time, the crystallinity of the AZO films deposited on GaAs SWGs was enhanced, which leaded to the decrease of the effective resistivity up to $\sim 1.55 \times 10^{-3}$ Ω-cm at 100 min. The wetting behavior of a water droplet on the surface of samples was also studied.

1. Introduction

Gallium arsenide (GaAs) has been widely used in devices such as laser diodes, light emitting diodes, photodetectors, and solar cells [1,2]. However, the reflectivity of GaAs at the surface is very high due to the Fresnel reflection caused by its high refractive index. Efficient antireflection coatings (ARCs) are often needed to suppress Fresnel reflection losses. Recently, the periodic subwavelength gratings (SWGs) have been exploited as an alternative of conventional thin-film ARCs [3–6]. In particular, the SWGs can efficiently reduce the surface reflections in the broadband and wide-incident-angle spectral range because a linear and continuous graded-refractive-index profile between air and the semiconductor material can be provided [7,8]. Moreover, it was reported that the nanostructures can self-clean any dirt and dust particles on the device surface when they have a hydrophobic property [9].

On the other hand, Al-doped zinc oxide (AZO) is of great interest in many device applications as transparent electrodes due to its good electrical and optical properties as well as the low cost and non-toxicity [10–13]. The AZO films also can be used as an ARC on the semiconductor materials with a high refractive index because of its intermediate refractive index (i.e. $n_{AZO} \sim 2$). However, although the ZnO (or AZO) films deposited on flat GaAs substrates were reported [14,15], there has been little behavioral research on the coverage of AZO films on GaAs SWGs. Thus, the studies on the characteristics of AZO films deposited onto periodic GaAs SWGs are required for photovoltaic device applications. In this work, we investigated the effect of AZO films with different thicknesses deposited onto periodic GaAs SWG structures, fabricated by laser interference lithography, inductively coupled plasma (ICP) etching, and rf magnetron sputtering, on the wetting behavior of a water droplet on the surface of samples as well as their structural, optical, and electrical properties.

2. Experimental details

Fig. 1 shows the schematic diagram of the fabrication procedure of AZO deposited GaAs SWG structures by the sputtering method. To fabricate the cone-shaped SWG structures on GaAs substrates, single-side polished, semi-insulating, and undoped (1 0 0) GaAs wafers were used. The 2D periodic photoresist nanopatterns with a 6-fold hexagonal symmetry were formed on the GaAs substrates (1.5 cm × 1.5 cm) by the laser interference lithography (Ar laser: $\lambda \sim 363.8$ nm). And then, the SWG structure was fabricated on GaAs substrates by using an ICP (Plasmalab System 100, Oxford) etcher. The fabrication details of the cone-shaped GaAs SWG structure were described in our previous work [5]. In order to cover the optimized AZO films on fabricated GaAs SWGs, the rf magnetron sputtering system (KVS-2000L, Korea Vac. Tech. Ltd.) was employed. The sputtering source target of 99.999% purity 2 wt.% Al_2O_3-doped zinc oxide (AZO) was used. Initially, the vacuum chamber was pumped to a 10^{-6} Torr base pressure. The

* Corresponding author.
E-mail address: jsyu@khu.ac.kr (J.S. Yu).

0025-5408/$ – see front matter © 2012 Elsevier Ltd. All rights reserved.
http://dx.doi.org/10.1016/j.materresbull.2012.04.090

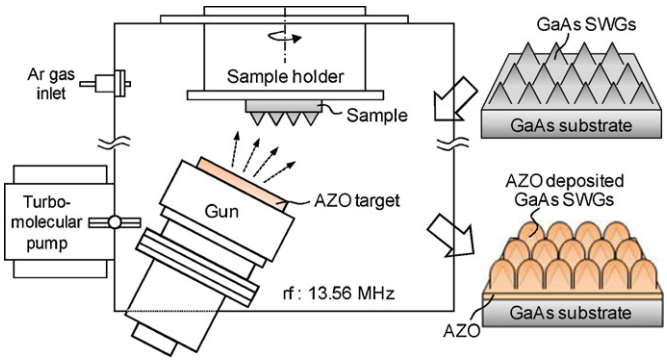

Fig. 1. Schematic diagram of the fabrication procedure of AZO deposited GaAs SWG structures by the sputtering method.

deposition process was carried out with 30 sccm Ar, 150 W rf power, 10 mTorr pressure at room temperature. The distance between the target and the sample was 20 cm. For good uniformity, the samples were rotated with 10 rpm during the deposition. The film deposition rate was kept at ~5 nm/min by using a quartz crystal thickness monitoring system. The AZO films on GaAs SWG structures were prepared at 40, 60, and 100 min.

After the deposition, all the samples were annealed at 420 °C under N_2 environment for 2 min by using a rapid thermal annealing system (RTA, KVR-2000, Korea Vac. Tech. Ltd.). The surface morphologies and deposited profiles of AZO deposited GaAs SWG structures were observed by using a scanning electron microscope (SEM, S-4700, Hitachi). The crystallinity was analyzed by using a X-ray diffractometer (XRD, M18XHF-SRA, Mac Science) with a monochromated Cu Kα line (λ = 0.154178 nm). The optical reflectance was measured by using a UV–vis-NIR spectrophotometer (Cary 5000, Varian). The composition of the deposited AZO films on GaAs SWG structures was determined by using an energy dispersive spectroscopy (EDS, 7060 eXL linked with Stereoscan 440, Oxford/Leica Cambridge). The effective electrical properties were also measured by using a Hall effect measurement system (HL5500PC, Accent). The contact angles were measured after putting a water droplet on the surface of samples by using a contact angle measurement system (Phoenix-300, SEO Co., Ltd.) and the results were averaged by the measured values at the three different positions.

3. Results and discussion

Cross-sectional SEM images of (i) the fabricated GaAs SWG structure and the AZO deposited GaAs SWG structures at (ii) 40 min, (iii) 60 min, and (iv) 100 min are depicted in Fig. 2(a). Each inset shows the oblique-view SEM image of the corresponding structures. For the fabricated GaAs SWG structure, the cone-shaped grating structure was well formed on the GaAs substrate, resulting in an effectively graded refractive index profile with an arch curve [7]. The height and period of SWGs were observed to be ~330 nm and ~320 nm, respectively. As the AZO deposition time was increased up to 60 min, the SWGs were gradually changed into closely-packed nanopillars with a hemispherical top. At 40 min, the AZO deposited GaAs SWG structure has an effective refractive index profile close to a linear gradient from air to the substrate. Clearly, this is attributed to the parabolic shape of the AZO deposited GaAs SWG [7,8]. In contrast, at 100 min, the surface of the AZO deposited GaAs SWGs became a flat film-like structure with molar-shaped nanopillars, which has a more abrupt change in the effective refractive index between air and the flat top of the structure. Also, the height of AZO deposited GaAs SWGs got

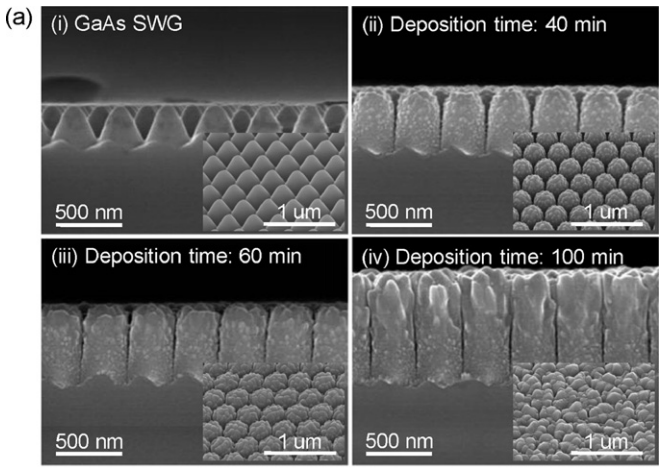

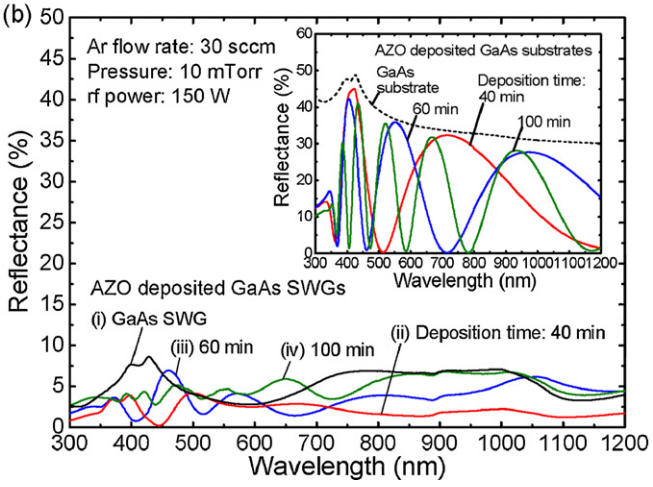

Fig. 2. (a) Cross-sectional SEM images and (b) optical reflectance characteristics of (i) the fabricated GaAs SWG structure and the AZO deposited GaAs SWG structures at (ii) 40 min, (iii) 60 min, and (iv) 100 min. The insets of (a) show the oblique-view SEM images of the corresponding structures. For comparison, the reflectance spectra of GaAs substrate and AZO deposited GaAs substrates at different deposition times are also shown in (b).

gradually higher with increasing the deposition time, exhibiting ~520 nm at 40 min, ~630 nm at 60 min, and ~830 nm at 100 min, respectively.

Fig. 2(b) shows the reflectance characteristics of the fabricated GaAs SWG structure and the AZO deposited GaAs SWG structures at different deposition times. For comparison, the reflectance spectra of GaAs substrate and AZO deposited GaAs substrates at different deposition times are also shown in the inset. The bare GaAs substrate exhibits the high reflectance spectrum of >30% due to its high refractive index value at 300–1200 nm. For the GaAs SWG structure, the reflectance was significantly reduced compared to the GaAs substrate because of the graded refractive index profile, indicating an average reflectance of ~5.2%. For the AZO deposited GaAs SWG structures, the reflectance was much lower than those of the AZO deposited GaAs substrates, which was also lower than that of the GaAs SWG structure. This can be explained by the fact that the more graded refractive index distribution from air ($n_{air} = 1$) to the GaAs ($n_{GaAs} \sim 3.8$) via the AZO with an intermediate refractive index ($n_{AZO} \sim 2$) is formed [16]. Additionally, the increased height of the AZO deposited GaAs SWG structure helps to reduce the reflectance [4]. As the deposition time was increased, the reflectance of the AZO deposited GaAs SWGs was

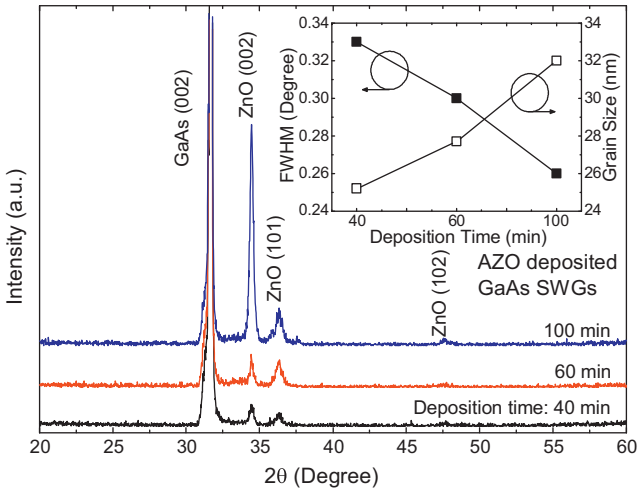

Fig. 3. XRD patterns of the AZO deposited GaAs SWG structures at different deposition times. The inset shows the FWHM value of XRD (0 0 2) peak and the grain size of the corresponding structures versus deposition time.

gradually increased at 300–1200 nm and they had more oscillations in the reflectance spectrum due to the constructive or destructive interference. It is noticeable that the AZO deposited GaAs SWG structures are changed from the parabolic grating structure into the flat molar-like film. But, at 100 min, the reflectance spectrum still exhibited the lower values than ~6.8%. At 40 min, the maxima values in the reflectance spectrum were below than ~4.2%, which leads to the lowest average reflectance of ~2.1%.

Fig. 3 shows the XRD patterns of the AZO deposited GaAs SWG structures at different deposition times. The full width at half maximum (FWHM) value of XRD (0 0 2) peak and the grain size of the corresponding structures as a function of deposition time are also shown in the inset. The peaks at 2θ values of 34.4, 36.3, and 47.5° correspond to the (0 0 2), (1 0 1), and (1 0 2) crystal planes of the crystalline ZnO thin film with a wurtzite structure, respectively. Particularly, the intense and sharp (0 0 2) diffraction peak indicates that the AZO film was well grown with a *c*-axis orientation, even on the GaAs SWG structure. The (1 0 0) ZnO peak at $2\theta \sim 31.8°$ may be covered by the strong (002) GaAs peak at $2\theta \sim 31.6°$. The FWHM value was decreased from 0.33° at 40 min to 0.26° at 100 min. The mean grain size, D, can be calculated by employing the well-known Scherrer formula, i.e. $D = 0.9\lambda/(\beta\cos\theta)$, where λ is the wavelength of the X-ray, β is the FWHM of the (0 0 2) diffraction peak, and θ is the diffractive angle. According to this formula, the mean grain sizes at deposition times of 40, 60, and 100 min were 25.2, 27.7, and 32 nm, respectively. This results from the increase of the AZO film thickness on GaAs SWGs with increasing the deposition time. Thus, the XRD measurements confirm that the crystallinity is improved and the mean grain size becomes larger by the increase of the AZO film thickness on GaAs SWGs, which are similar to the previous results [13].

Table 1
Composition of AZO films deposited on GaAs SWG structures at different deposition times.

Samples (deposition time)	Al (wt.%)	Zn (wt.%)	O (wt.%)
40 min	2.03	41.32	56.65
60 min	2.09	45.1	52.82
100 min	2.3	52.83	44.87

Table 2
Effective electrical properties such as resistivity, carrier concentration, and Hall mobility of the AZO films deposited on GaAs SWG structures at different deposition times.

Samples (deposition time)	Resistivity ($\times 10^{-3}\,\Omega$-cm)	Carrier concentration ($\times 10^{20}\,cm^{-3}$)	Hall mobility ($cm^2\,V^{-1}\,s^{-1}$)
40 min	7.34	4.06	2.1
60 min	5.21	4.98	3.04
100 min	1.55	7.63	5.28

The composition of AZO films deposited on GaAs SWG structures at different deposition times is displayed in Table 1. The amount of Al was almost not changed from 2.03 to 2.3 wt.% though the deposition time was increased from 40 to 100 min, which is similar in composition to the Al_2O_3 (i.e. 2 wt.%) source target. In contrast, the Zn and O contents were increased from 41.32 to 52.83 wt.% and decreased from 56.65 to 44.87 wt.% with increasing the deposition time from 40 to 100 min, respectively. This is attributed to the preferential sputtering of Zn atoms [17].

In order to obtain the effective electrical properties of AZO films deposited on GaAs SWGs, the indium contacts were used on the squared sample surface in the Van der Pauw geometry. The effective electrical properties of the AZO films deposited on GaAs SWG structures at different deposition times are summarized in Table 2. The effective resistivity was decreased from $7.34 \times 10^{-3}\,\Omega$-cm at 40 min to $1.55 \times 10^{-3}\,\Omega$-cm at 100 min. This is probably ascribed to the enhanced crystallinity and larger mean grain size by the increased thickness of the AZO film, which results in the increase of the carrier concentration and Hall mobility. With increasing the deposition time from 40 to 100 min, the carrier concentration and Hall mobility were increased from $4.06 \times 10^{20}\,cm^{-3}$ and $2.1\,cm^2\,V^{-1}\,s^{-1}$ to $7.63 \times 10^{20}\,cm^{-3}$ and $5.28\,cm^2\,V^{-1}\,s^{-1}$, respectively.

Fig. 4(a) shows the photographs of samples for (i) GaAs substrate, (ii) GaAs SWG, and (iii) AZO deposited GaAs SWG at 40 min. The characters in the LCD monitor were reflected at the surface of the GaAs substrate. However, the fabricated GaAs SWG and AZO deposited GaAs SWG samples showed the dark black surfaces without any reflected characters. Absolutely, this fact confirms their antireflective properties in Fig. 2(b). The photographs of water droplets with a contact angle (θ_c) on the surface of GaAs substrate, GaAs SWG, and AZO deposited GaAs SWG structures at 40, 60, and 100 min are shown in Fig. 4(b). The cone-shaped GaAs SWG exhibited a hydrophobic surface with the contact angle of 102° while the surface of GaAs substrate was a hydrophilic with the contact angle of 41°. This may be ascribed to the nanoscale roughness on the surface, which can be explained by the Cassie–Baxter theory [18]. The surface wettability of AZO deposited GaAs SWG structures was strongly affected by the deposition time of the AZO film. At 40 min of deposition time, the AZO deposited GaAs SWG structure had a hydrophobic surface of $\theta_c \sim 109°$, which was larger than that of the GaAs SWG. This can be explained by the fact that the AZO has a lower surface energy than that of the GaAs [19]. At the deposition times longer than 60 min, while the surface of the structures exhibited hydrophilic properties (i.e. $\theta_c \sim 72°$ at 60 min and $\theta_c \sim 53°$ at 100 min, respectively). This reason is because the wettability is determined by the surface morphology of the AZO deposited GaAs SWG structures at different deposition times. In the case of AZO deposited GaAs SWG structure at 40 min, it can be used for the self-cleaning purpose which removes the dust particles on the device surface in real environments. From these results, there is a compromise between the optical and electrical properties as well as the

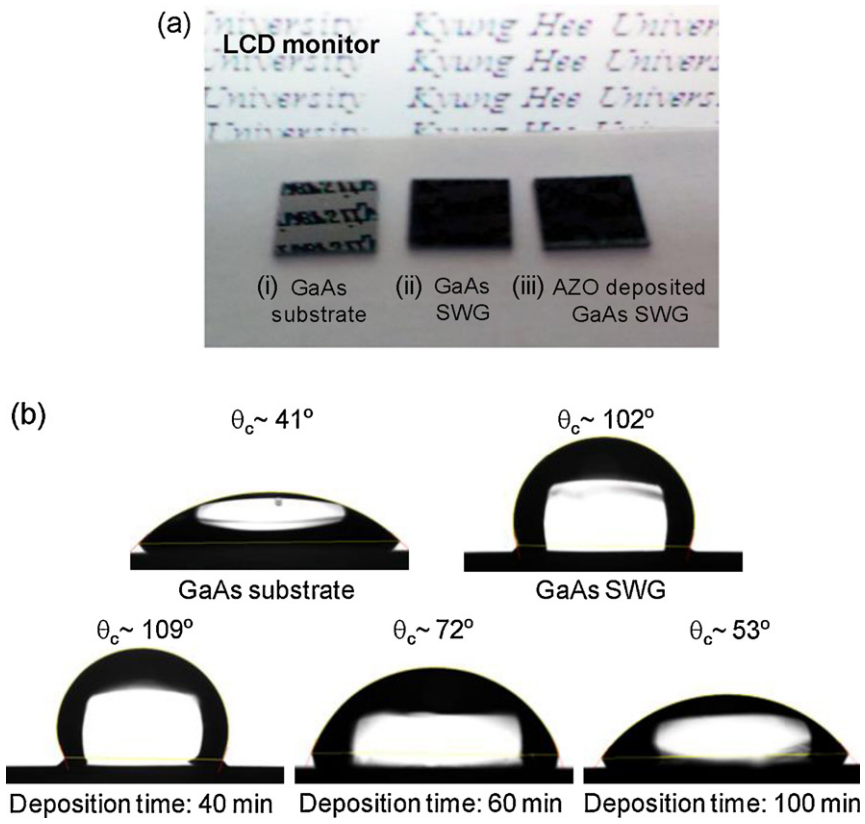

Fig. 4. (a) Photographs of samples for (i) GaAs substrate, fabricated, (ii) GaAs SWG, and (iii) AZO deposited GaAs SWG at 40 min and (b) water droplets with a contact angle on the surface of GaAs substrate, GaAs SWG, and AZO deposited GaAs SWG structures at 40, 60, and 100 min.

wetting behavior at the surface of AZO deposited GaAs SWG structures to achieve high-performance photovoltaic devices.

4. Conclusion

The structural, optical, and electrical properties as well as the wetting behavior on the surface of AZO deposited GaAs SWG structures were investigated. With increasing the deposition time, the shape of the AZO deposited GaAs SWGs was changed from parabolic structure with a hemispherical top at 40 min into flat film-like one with molar-shaped nanopillars at 100 min. For AZO deposited GaAs SWGs, the reflectance spectra were below ~6.8% at 300–1200 nm. Especially, for the AZO deposited GaAs SWG at 40 min, the average reflectance exhibited a value of ~2.1%. Whereas the structure deposited at 40 min had a hydrophobic surface of $\theta_c \sim 109^\circ$, the other samples deposited at times longer than 60 min exhibited a hydrophilic property. Also, the effective resistivity was decreased from $7.34 \times 10^{-3}\ \Omega$-cm at 40 min to $1.55 \times 10^{-3}\ \Omega$-cm at 100 min due to the improved crystallinity of the AZO films deposited on GaAs SWGs.

Acknowledgments

This research was supported by Basic Science Research Program through the National Research Foundation of Korea (NRF) funded by the Ministry of Education, Science and Technology (MEST) (No. 2011-0026393 and No. 2011-0031508).

References

[1] S.I. Tsintzos, N.T. Pelekanos, G. Konstantinidis, Z. Hatzopoulos, P.G. Savvidis, Nature 453 (2008) 372–375.
[2] T. Takamoto, M. Kaneiwa, M. Imaizumi, M. Yamaguchi, Prog. Photovolt: Res. Appl. 13 (2005) 495–511.
[3] J.W. Leem, Y.M. Song, Y.T. Lee, J.S. Yu, Appl. Phys. B 100 (2010) 891–896.
[4] S.A. Boden, D.M. Bagnall, Appl. Phys. Lett. 93 (2008) 133108.
[5] Y.M. Song, S.Y. Bae, J.S. Yu, Y.T. Lee, Opt. Lett. 34 (2009) 1702–1704.
[6] Y.M. Song, S.J. Jang, J.S. Yu, Y.T. Lee, Small 6 (2010) 984–987.
[7] D.G. Stavenga, S. Foletti, G. Palasantzas, K. Arikawa, Proc. R. Soc. B 273 (2006) 661–667.
[8] J.W. Leem, D.H. Joo, J.S. Yu, Sol. Energy Mater. Sol. Cells 95 (2011) 2221–2227.
[9] J. Zhu, C.M. Hsu, Z. Yu, S. Fan, Y. Cui, Nano Lett. 10 (2010) 1979–1984.
[10] L.J. Li, H. Deng, L.P. Dai, J.J. Chen, Q.L. Yuan, Y. Li, Mater. Res. Bull. 43 (2008) 1456–1462.
[11] F. Ahmed, S. Kumar, N. Arshi, M.S. Anwar, B.H. Koo, C.G. Lee, Funct. Mater. Lett. 4 (2011) 1–5.
[12] L. Guo, L.L. Kerr, Funct. Mater. Lett. 3 (2010) 279–283.
[13] C.H. Huang, H.L. Cheng, W.E. Chang, M.S. Wong, J. Electrochem. Soc. 158 (2011) H510–H515.
[14] M.Y. Han, J.H. Jou, Thin Solid Films 260 (1995) 58–64.
[15] J.I. Son, J.H. Shim, N.H. Cho, Met. Mater. Int. 17 (2011) 99–104.
[16] J.W. Leem, Y.M. Song, J.S. Yu, Opt. Express 19 (2011) A1155–A1164.
[17] L.S. Dorneles, D. O'Mahony, C.B. Fitzgerald, F. McGee, M. Venkatesan, I. Stanca, J.G. Lunney, J.M.D. Coey, Appl. Surf. Sci. 248 (2005) 406–410.
[18] A.B.D. Cassie, S. Baxter, Trans. Faraday Soc. 40 (1944) 546–551.
[19] J.W. Leem, Y.M. Song, J.S. Yu, Nanotechnology 22 (2011) 485304.